

The first bifurcation point for Delaunay nodoids

Wayne Rossman

Abstract: We give two numerical methods for computing the first bifurcation point for Delaunay nodoids. With regard to methods for constructing constant mean curvature surfaces, we conclude that the bifurcation point in the analytic method of Mazzeo-Pacard is the same as a limiting point encountered in the integrable systems method of Dorfmeister-Pedit-Wu.

1. INTRODUCTION

Delaunay surfaces in Euclidean 3-space

$$\mathbf{R}^3 = \{(x_1, x_2, x_3) \mid x_j \in \mathbf{R}\}$$

are constant mean curvature (CMC) surfaces of revolution, and they are translationally periodic. By a rigid motion and homothety of \mathbf{R}^3 we may place the Delaunay surfaces so that their axis of revolution is the x_1 -axis and their constant mean curvature is $H = 1$ (henceforth we assume this).

We consider the profile curve in the half-plane $\{(x_1, 0, x_3) \in \mathbf{R}^3 \mid x_3 > 0\}$ that gets rotated about the x_1 -axis to trace out a Delaunay surface. This curve alternates periodically between maximal and minimal heights (with respect to the positive x_3 direction), which we refer to as the bulge radius and the neck radius, respectively, of the Delaunay surface. Let us denote the neck radius by r .

Delaunay surfaces come in two 1-parameter families: one is a family of embedded surfaces called *unduloids* that can be parametrized by the neck radius $r \in (0, 1/2]$; the other is a family of nonembedded surfaces called *nodoids* that can be parametrized by the neck radius $r \in (0, \infty]$. For unduloids, $r = 1/2$ gives the round cylinder. For both unduloids and nodoids, the limiting degenerate surface as $r \rightarrow 0$ is a chain of tangent spheres of radii 1 centered along the x_1 -axis.

In this paper we shall be concerned with nodoids. We will see that a common bifurcation point for Delaunay nodoids is encountered in the following two distinctly different approaches for constructing CMC surfaces:

- (1) Using analytic techniques, Mazzeo and Pacard [12] showed existence of a finite value r_0 so that for neck radii $r < r_0$ the nodoids are nonbifurcating, and for $r > r_0$ the nodoids can bifurcate. They showed that bifurcating nodoids deform smoothly through families of CMC surfaces that are of bounded distance from a fixed line yet are not surfaces of revolution. They also gave an analytic gluing construction for CMC surfaces with asymptotically Delaunay ends (i.e. each end converges¹ to an end of a Delaunay surface) that works only when each end converges to a nonbifurcating Delaunay end, that is, each end converges either to an unduloid, or to a nodoid with neck size less than r_0 . Their gluing construction involves adding ends of neck radii r close to zero to a preexisting CMC surface. Of course those r close to zero are less than r_0 , but the construction also requires that all the asymptotically nodoid ends of the preexisting surface satisfy $r < r_0$. So the surfaces constructed will necessarily have asymptotic neck radii $r < r_0$ at all asymptotically nodoidal ends. There are a number of other gluing constructions along these lines for making CMC surfaces, and they always involve the Delaunay ends being nonbifurcating. (See the works of Kusner, Mazzeo, Pacard, Pollack, Ratzkin [11], [13], [14], [17] for more on this.)

Mazzeo and Pacard gave a clear reason for the existence of this bifurcation point r_0 , in terms of the existence of nontrivial nullity for a particular Jacobi operator associated to the second variation formula for Delaunay surfaces, but they did not compute the precise value of r_0 .

- (2) Using integrable systems techniques developed by Dorfmeister, Pedit and Wu in [7], Dorfmeister, Wu [8] and Schmitt [19] (see also [9]) constructed genus 0 CMC surfaces with three asymptotically Delaunay ends. In [8] the construction was restricted to surfaces with asymptotically unduloidal ends, because such ends are embedded. However, the construction in [19] and [9] includes asymptotically nodoidal ends as well. The construction begins with the selection of

¹Here "converges" means uniform convergence on compact subsets, in C^∞ topology.

a certain "DPW potential", and the DPW potential in [19] and [9] fails to exist when some nodoidal end has an asymptotic neck radius greater than $1/2$. Furthermore, the arguments in [19] and [9] showing that each end converges to a Delaunay surface work only when the limiting Delaunay surface is an unduloid, or is a nodoid with neck size less than $1/2$. This suggests that there is possibly some obstruction in the DPW approach to CMC surfaces with Delaunay ends that occurs only for asymptotically nodoidal ends with asymptotic neck radii at least $1/2$.

In the construction in [19] and [9], this limiting value $1/2$ appears explicitly, but the underlying reasons for its appearance are left unexplained.

It is natural to ask if the bifurcation radius r_0 in the first approach coincides with the limiting value $1/2$ in the second approach. The purpose of this article is to numerically confirm this:

Numerical result. The bifurcation radius r_0 is equal to $1/2$.

This result is of interest with respect to both approaches above. For the first approach, it gives the exact (previously unknown) value for r_0 . For the second approach, it provides a reason (via the bifurcation properties shown by Mazzeo and Pacard) for the existence of the previously mysterious limiting value $1/2$.

In fact, we shall show a stronger numerical result about the first eigenvalue of a particular operator, for which the above numerical result is an immediate corollary.

To provide added confidence in the accuracy of our numerical arguments, we give two different independent algorithms for showing that $r_0 = 1/2$ (and for showing the stronger numerical result as well). The first method involves using an ordinary differential equation (ODE) solver and symmetry properties of the first eigenfunction. The second method requires more machinery, the basic tool being the Rayleigh quotient characterization for eigenvalues of a self-adjoint operator. It involves numerical integration of smooth bounded functions of a single variable on a finite interval, and it has the advantage of also giving estimates for other eigenvalues beyond the first one.

2. PARAMETRIZING NODOIDS

Let (x_1, x_2, x_3) be the usual rectangular coordinates for \mathbf{R}^3 . Consider a Delaunay nodoid with the x_1 -axis as its axis and with constant mean curvature $H = 1$. Let

$$(x(t), z(t)) , \quad t \in \mathbf{R}$$

be a parametrization of the profile curve of the nodoid in the x_1x_3 -plane, and so the surface can now be parametrized by

$$\mathcal{D}(t, \theta) = (x(t), z(t) \cos \theta, z(t) \sin \theta) , \quad t \in \mathbf{R} , \quad \theta \in [0, 2\pi) .$$

Suppose further that the parameter t is chosen to make the mapping $\mathcal{D}(t, \theta)$ conformal with respect to the coordinates (t, θ) . Let $t = a$ and $t = b$ be values at which the nodoid achieves two adjacent necks, i.e. $z(t)$ has local minima at both $t = a$ and $t = b$ equal to the neck radius r but at no $t \in (a, b)$. Conformality implies that the first fundamental form is

$$ds^2 = ((x')^2 + (z')^2)dt^2 + z^2d\theta^2 = \rho^2(dt^2 + d\theta^2) ,$$

with

$$\rho^2 = (x')^2 + (z')^2 = z^2 .$$

The second fundamental form is then

$$\frac{1}{z}(x''z' - z''x')dt^2 + x'd\theta^2 ,$$

and so the coordinates (t, θ) are curvature line coordinates, that is, the coordinates are isothermic. Furthermore, the mean curvature $H = 1$ implies

$$2z^3 - z'x'' + x'z'' - zx' = 0 .$$

This has a first integral, that is, using $z^2 = (x')^2 + (z')^2$ and $zz' = x'x'' + z'z''$, it is equivalent to

$$(4x' - 4z^2)' = 0 .$$

Thus

$$(1) \quad m = 4x' - 4z^2$$

is satisfied for some t -independent constant m . Because there are points on a nodoid where $x' = 0$, we have

$$m < 0 .$$

In fact, $m \in (-\infty, 0)$ is a parameter that determines the full family of Delaunay nodoids. Equation (1) can also be established using a homology invariant on CMC surfaces called the weight, as explained by Korevaar, Kusner and Solomon in [10]. We define m as the mass²:

Definition 1. Given a nodoid $\mathcal{D}(t, \theta)$ parametrized as above satisfying Equation (1), we say that m is the *mass* of the nodoid $\mathcal{D}(t, \theta)$.

Equation (1) implies

$$(2) \quad z' = \pm \sqrt{z^2 - \left(\frac{m}{4} + z^2\right)^2}, \quad m < 0 .$$

Then x' is determined by z via Equation (1), so x is determined up to translation, as expected.

Equation (2) has the solution

$$z = -2B \cdot \text{JacobiSN}\left(\chi(t), \frac{B^2}{A^2}\right), \quad \chi(t) = 2iA \left(t - b - \frac{i \cdot \text{InverseJacobiSN}[1, \frac{B^2}{A^2}]}{2a}\right)$$

in the notation of Mathematica, where $B = \frac{-1}{4}(\sqrt{1-m} - 1)$ and $A = \frac{1}{2} - B$. From this we can see that the minimum (neck radius) of z is

$$(3) \quad r = \sqrt{\frac{1 - \frac{m}{2} - \sqrt{1-m}}{2}}$$

at $t = a$ and $t = b$, the maximum (bulge radius) of z is

$$\sqrt{\frac{1 - \frac{m}{2} + \sqrt{1-m}}{2}}$$

at $t = \frac{a+b}{2}$, and $x' = 0$ and $z = \sqrt{\frac{-m}{4}}$ at both $t = \frac{3a+b}{4}$ and $t = \frac{a+3b}{4}$.

The Gaussian curvature K is determined by ds^2 as

$$K = \frac{-1}{\rho^2} \Delta(\log \rho),$$

where

$$(4) \quad \Delta = \frac{\partial^2}{\partial t^2} + \frac{\partial^2}{\partial \theta^2}$$

is the standard Euclidean Laplacian operator.

We now introduce a function V that will be used in the second variational formula later. We set

$$V = (4 - 2K)\rho^2 .$$

It can be computed that

$$(5) \quad V = z^{-2}(2z^4 + \frac{1}{8}m^2) .$$

Note that $V = V(t)$ is a function of t , and is independent of θ .

Lemma 1. *The function $V = V(t)$ has the following symmetries:*

$$V(\ell + t) = V(\ell - t) \quad \forall \ell \in \{a, \frac{3a+b}{4}, \frac{a+b}{2}, \frac{a+3b}{4}, b\} .$$

Furthermore,

$$-m \leq V \leq 2 - m \quad \forall t \in \mathbf{R} .$$

² m is also sometimes called the "weight" or "flux".

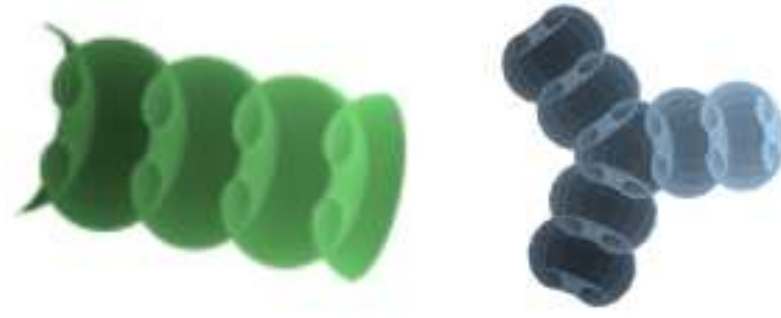


FIGURE 1. A nodoid and a CMC surface with three ends asymptotic to nodoids. One of two halves of each surface is shown here. (Computer graphics made using N. Schmitt's cmclab software [20] and K. Polthier's Javaview software [16].)

Proof. We will show that $V(a+t) = V(a-t)$ and $V(\frac{3a+b}{4}+t) = V(\frac{3a+b}{4}-t)$, and then all other symmetries in the lemma will immediately follow. Because $z(t)$ itself has the symmetry $z(a+t) = z(a-t)$, clearly also $V(a+t) = V(a-t)$ by Equation (5). We now show that $V(\frac{3a+b}{4}+t) = V(\frac{3a+b}{4}-t)$: We first note that

$$\frac{z'(t)}{z(t)} = 2iA \frac{\text{JacobiCN}(\chi(t), \frac{B^2}{A^2}) \text{JacobiDN}(\chi(t), \frac{B^2}{A^2})}{\text{JacobiSN}(\chi(t), \frac{B^2}{A^2})},$$

and so

$$(6) \quad \frac{z'(\frac{3a+b}{4}+t)}{z(\frac{3a+b}{4}+t)} = \frac{z'(\frac{3a+b}{4}-t)}{z(\frac{3a+b}{4}-t)}.$$

Substituting $m^2/8 = (2-m)z^2 - 2z^4 - 2(z')^2$ from Equation (2) into Equation (5), we have

$$(7) \quad V(t) = 2 - m - 2 \left(\frac{z'}{z} \right)^2,$$

Then by Equation (6), we have $V(\frac{3a+b}{4}+t) = V(\frac{3a+b}{4}-t)$. Equation (7) also implies that $V \leq 2 - m$ for all t .

To see that $V \geq -m$ for all t , we simply consider $V = 2\zeta + \frac{m^2}{8}\frac{1}{\zeta}$ as a function of $\zeta = z^2 > 0$. Elementary calculus gives that $2\zeta + \frac{m^2}{8\zeta} \geq -m$ for all $\zeta > 0$. \square

3. SECOND VARIATION FOR NODOIDS

We now consider an arbitrary volume-preserving periodic smooth variation of the surface, that is, a family of surfaces $\mathcal{D}_s(t, \theta)$ that is

- (1) smooth with respect to $s \in (-\epsilon, \epsilon)$ for some $\epsilon > 0$,
- (2) an immersion with respect to the coordinates (t, θ) for any fixed $s \in (-\epsilon, \epsilon)$,
- (3) satisfying $\mathcal{D}_0(t, \theta) = \mathcal{D}(t, \theta)$ for all $t \in \mathbf{R}$ and $\theta \in [0, 2\pi)$,
- (4) with compact regions bounded by the surfaces $\mathcal{D}_s(t, \theta)$, $t \in [a, b]$, $\theta \in [0, 2\pi)$ and the two disks

$$D_a = \{(x(a), x_2, x_3) \mid x_2^2 + x_3^2 \leq (z(a) + \mathcal{O}(s))^2\},$$

$$D_b = \{(x(b), x_2, x_3) \mid x_2^2 + x_3^2 \leq (z(b) + \mathcal{O}(s))^2\}$$

having the same volume for all $s \in (-\epsilon, \epsilon)$,

- (5) periodic with the same period for all $s \in (-\epsilon, \epsilon)$, i.e. $\mathcal{D}_s(t_1, \theta) = \mathcal{D}_s(t_2, \theta)$ for all $s \in (-\epsilon, \epsilon)$ and all $t_2 - t_1$ an integer multiple of $b - a$.

Let \vec{N} denote a unit normal vector to $\mathcal{D}_0(t, \theta)$. We define the function u by

$$u = u(t, \theta) = \left\langle \frac{d}{ds} \mathcal{D}_s(t, \theta) \Big|_{s=0}, \vec{N} \right\rangle \in \mathcal{F}.$$

The volume-preserving condition 4. above implies

$$\int_a^b \int_0^{2\pi} u \rho^2 d\theta dt = 0.$$

Definition 2. We will call the compact portion $\mathcal{D}(t, \theta), t \in [a, b], \theta \in [0, 2\pi)$ a *fundamental piece* of the nodoid.

Let $A(s)$ denote the area of the surface $\mathcal{D}_s(t, \theta)$ for $t \in [a, b], \theta \in [0, 2\pi)$. Because the nodoid is CMC $H = 1$, the first variation formula for a fundamental piece is

$$\frac{d}{ds} A(s) \Big|_{s=0} = \int_a^b \int_0^{2\pi} u \rho^2 d\theta dt = 0.$$

Thus it is the second variation formula for volume-preserving variations (see [1])

$$\begin{aligned} \frac{d^2}{ds^2} A(s) \Big|_{s=0} &= \int_a^b \int_0^{2\pi} u (-\Delta_{ds^2} u - (4 - 2K)u) \rho^2 d\theta dt \\ &= \int_a^b \int_0^{2\pi} u \cdot \mathcal{L}(u) d\theta dt = 0, \quad \mathcal{L}(u) := -\Delta u - Vu, \end{aligned}$$

with Δ_{ds^2} (respectively Δ) the Laplace-Beltrami operator determined by ds^2 (respectively the Euclidean Laplacian as in (4)), that will determine if the variation increases or decreases area (when this formula is nonzero).

4. SPHERICAL HARMONICS

We now consider the eigenvalue problem for \mathcal{L} . We first introduce the function space

$$\mathcal{F} = \{u = u(t, \theta) \in C^\infty(t, \theta) \mid u(t_1, \theta) = u(t_2, \theta) \text{ for } t_1 - t_2 \in (b - a) \cdot \mathbf{Z}\}.$$

The eigenvalue problem is to find $u \in \mathcal{F}$ and $\lambda \in \mathbf{R}$ such that

$$(8) \quad \mathcal{L}(u) = \lambda u.$$

Let us decompose such an eigenfunction u into its spherical harmonics: $u = u(t, \theta)$ can be written as

$$u = u_0(t) + \sum_{j \geq 1} (u_{j,+}(t) \cdot \cos(j\theta) + u_{j,-}(t) \cdot \sin(j\theta)),$$

where $u_0(t)$, $u_{j,+}(t)$ and $u_{j,-}(t)$ are periodic functions of t , that is, they lie in the smaller function space

$$\hat{\mathcal{F}} = \mathcal{F} \cap \{u = u(t, \theta) \mid \frac{\partial}{\partial \theta} u \equiv 0\},$$

i.e. those functions in \mathcal{F} that are independent of θ . Defining the operators

$$\mathcal{L}_j = -\frac{\partial^2}{\partial t^2} - V + j^2$$

for $j \in \mathbf{Z}^+ \cup \{0\}$ on the function space $\hat{\mathcal{F}}$, the relation (8) gives also that

$$\mathcal{L}_0(u_0) = \lambda u_0, \quad \mathcal{L}_j(u_{j,\pm}) = \lambda u_{j,\pm}$$

for all $j \geq 1$. So the following lemma is immediate:

Lemma 2. *A real number λ is an eigenvalue of \mathcal{L} , i.e. $\mathcal{L}(u) = \lambda u$ for some $u \in \mathcal{F}$, if and only if λ is also an eigenvalue of \mathcal{L}_j for at least one value of $j \in \mathbf{Z}^+ \cup \{0\}$, i.e. $\mathcal{L}_j(\hat{u}) = \lambda \hat{u}$ for some $\hat{u} \in \hat{\mathcal{F}}$ and some $j \in \mathbf{Z}^+ \cup \{0\}$.*

The following lemma is analogous to Proposition 4.4 in [12], but different notations were used there:

Proposition 3. *Both -1 and 0 are eigenvalues of \mathcal{L}_0 .*

Proof. We first show that 0 is an eigenvalue. Considering the vector $(1, 0, 0)$ as a constant vector field of \mathbf{R}^3 , the associated translational flow gives a periodic volume-preserving deformation \mathcal{D}_s of the nodoid $\mathcal{D} = \mathcal{D}_0$. Because this flow is actually a family of rigid motions, it is also area-preserving. It is a classical fact that the scalar product of the unit normal vector of a CMC surface with a Killing field is in the null-space of the Jacobi operator of the surface (see [6], page 196, or the proof of Theorem 2.7 in [2]). Hence, if $(1, 0, 0)$ is decomposed into $(1, 0, 0) = u\vec{N} + \vec{v}$ at each point of \mathcal{D} with $u\vec{N}$ normal to \mathcal{D} and \vec{v} tangent to \mathcal{D} , and with $u \in \hat{\mathcal{F}}$ and $|\vec{N}| = 1$, then $\mathcal{L}(u) = 0$. Since $u \in \hat{\mathcal{F}}$, it follows that 0 is an eigenvalue of \mathcal{L}_0 for any choice of $m < 0$. Also, by direct computation, we have $u = -z'/z$, and then using $(z')^2 = z^2 - (z^2 + m/4)^2$ and $z'' = z - 2z(z^2 + m/4)$, we have $\mathcal{L}_0(u) = 0$.

Now we show that -1 is an eigenvalue. Similarly to the previous case with eigenvalue 0, we now consider the vector $(0, 0, 1)$, producing a smooth vector field of \mathbf{R}^3 , whose associated translational flow again gives a periodic volume-preserving deformation \mathcal{D}_s of $\mathcal{D} = \mathcal{D}_0$ that is once again area-preserving. Now we decompose $(0, 0, 1) = u \sin \theta \vec{N} + \vec{v}$ at each point of \mathcal{D} with $u \sin \theta \vec{N}$ normal to \mathcal{D} and \vec{v} tangent to \mathcal{D} . Then $\mathcal{L}(u \sin \theta) = 0$, and $u \in \hat{\mathcal{F}}$ is an eigenfunction of \mathcal{L}_1 with eigenvalue 0. It follows that -1 is an eigenvalue of \mathcal{L}_0 for any choice of $m < 0$. Again, we could also see this by direct computation: we have $u = x'/z = z + m/(4z)$, and then using $(z')^2 = z^2 - (z^2 + m/4)^2$ and $z'' = z - 2z(z^2 + m/4)$, we have $\mathcal{L}_0(u) = -u$. \square

Both the operator \mathcal{L} on the function space \mathcal{F} and the operators \mathcal{L}_j on the function space $\hat{\mathcal{F}}$ are essentially self-adjoint, and hence standard functional analysis arguments (see [3] or [21] or [4] for example) give the following result:

Proposition 4. *Each of the operators \mathcal{L} on the function space \mathcal{F} and \mathcal{L}_j on the function space $\hat{\mathcal{F}}$ satisfy the following:*

- (1) *all eigenvalues are real, and there are a countably infinite number of them,*
- (2) *all eigenvalues are greater than some real constant,*
- (3) *the eigenvalues do not accumulate at any finite real value,*
- (4) *when written in increasing order, the eigenvalues increase to $+\infty$,*
- (5) *the eigenspace associated to each eigenvalue is finite dimensional,*
- (6) *the collection of eigenspaces spans the full function space.*

We refer to the eigenvalue that is less than all the others as the first eigenvalue. The second eigenvalue is the one that is less than all but the first eigenvalue. The third eigenvalue is the one that is less than all but the first and second eigenvalues, and so on.

The Courant nodal domain theorem, which is valid in our setting (see [5]), tells us that the number of nodal domains of the eigenfunction associated to the j 'th eigenvalue is at most j (here we are counting eigenvalues with multiplicity). In particular, any (not identically zero) eigenfunction associated to the first eigenvalue has at most one nodal domain, and this is equivalent to saying that it never attains the value zero. Furthermore, if the eigenspace associated to the first eigenvalue contained two linearly independent functions, then some linear combination of the two functions would be a not-identically-zero function that does become zero at some value of t . This would contradict the Courant nodal domain theorem. We conclude the following:

Proposition 5. *For both the operator \mathcal{L} defined on the function space \mathcal{F} and the operator \mathcal{L}_0 defined on the function space $\hat{\mathcal{F}}$, the eigenspace associated to the first eigenvalue is 1 dimensional. Furthermore, any not-identically-zero function in this eigenspace never attains the value zero.*

Remark. The eigenvalues -1 and 0 of \mathcal{L}_0 are actually the second and third eigenvalues of \mathcal{L}_0 . This was shown in [12] by counting the nodal domains of the corresponding eigenfunctions.

The first two operators \mathcal{L}_0 and \mathcal{L}_1 never give any nondegeneracy in the sense of [12]. The first bifurcation point (as in [12]) is defined as follows:

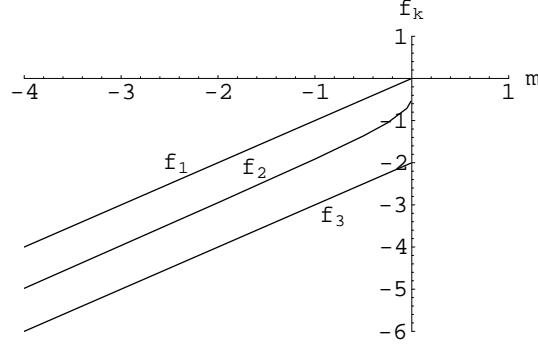


FIGURE 2. Plots of the functions $f_1 = m$, $f_3 = m - 2$ and $f_2 = \frac{-1}{b-a} \int_a^b V dt$. λ_0 is also a function of m , and Lemmas 6 and 8 imply that λ_0 must lie between f_2 and f_3 .

Definition 3. The *first bifurcation point* for Delaunay nodoids occurs at the value of $m < 0$ closest to zero for which \mathcal{L}_j for some $j \geq 2$ has a nonpositive eigenvalue, i.e.

$$\mathcal{L}_j u = \lambda u \text{ with } \lambda \leq 0 \text{ and } u \in \hat{\mathcal{F}} \text{ for some } j \geq 2.$$

This occurs at the largest value of m for which the first eigenvalue of \mathcal{L}_2 is zero, and is equivalent to the first eigenvalue λ_0 of \mathcal{L}_0 being -4 . This λ_0 can be computed using a minimum of the Rayleigh quotient ([3], [21], [4]):

$$(9) \quad \lambda_0 = \min_{u(t) \in \hat{\mathcal{F}} \setminus \{0\}} \frac{\int_a^b u(t) \mathcal{L}_0(u(t)) dt}{\int_a^b u(t)^2 dt}.$$

Remark. Bifurcation points are points where bifurcation actually occurs, that is, in any neighborhood of the Delaunay surface there are CMC surfaces that are not rotationally symmetric. What we have defined in Definition 3 is an "infinitesimal symmetry breaking point" where bifurcation might happen, because having zero as an eigenvalue of \mathcal{L}_2 is a necessary condition for the bifurcation to occur. However, because the multiplicity of the zero eigenvalue of \mathcal{L}_2 is one (see Proposition 5), and because the derivative of the first eigenvalue with respect to the parameter m is not zero (see the primary numerical result below), it turns out that the infinitesimal symmetry breaking point is an actual symmetry breaking point, i.e. a true bifurcation point [15].

Primary numerical result. For a nodoid of mean curvature 1 and mass m , the first eigenvalue λ_0 of \mathcal{L}_0 is

$$\lambda_0 = m - 1.$$

Hence the first bifurcation point for nodoids occurs when $m = -3$.

By the formula (3), $m = -3$ precisely when the neck radius is $r = 1/2$, thus the numerical result stated in the introduction is a direct corollary of this primary result just above.

We have two different numerical methods for checking this result. But first let us give two simple mathematically rigorous lemmas that support this numerical result. Both of these results are immediate from the Rayleigh quotient formulation for λ_0 above. The first lemma is also shown in Proposition 4.4 of [12], with different notations.

Lemma 6. For a nodoid of mean curvature 1 and mass m , the first eigenvalue λ_0 of \mathcal{L}_0 satisfies $m - 2 \leq \lambda_0 \leq m$.

Proof. Using the Rayleigh quotient characterization (9), this follows directly from the fact that $-m \leq V = V(t) \leq 2 - m$ for all t , as shown in Lemma 1. \square

We then immediately have:

Corollary 7. *For nodoids of mean curvature 1 and mass m , the first bifurcation point occurs for some m between -4 and -2 .*

Lemma 8. *For a nodoid of mean curvature 1 and mass m , the first eigenvalue λ_0 of \mathcal{L}_0 satisfies $\lambda_0 \leq \frac{-1}{b-a} \int_a^b V dt$.*

Proof. Inserting $u \equiv 1$ into the Rayleigh quotient in Equation (9), this lemma follows. \square

Numerically checking that $\frac{-1}{b-a} \int_a^b V dt$ is an increasing function of $m < 0$ that becomes -4 when (and only when) m is approximately -3.036 , we have the following corollary:

Preliminary numerical result. For nodoids of mean curvature 1 and mass m , the first bifurcation point occurs for some $m \geq -3.036$.

5. FIRST METHOD

In this and the next section we give two independent methods for numerically confirming our primary numerical result. The first method in this section is the simpler of the two.

We wish to solve

$$(10) \quad \frac{d^2}{dt^2} u + (V + \lambda)u = 0$$

for some $\lambda \in [m - 2, m]$ and some function $u = u(t) \in \hat{\mathcal{F}}$. If there is only one such value for $\lambda < -1$ in the range $[m - 2, m]$ (and we will see that this is the case), then this λ will be the first eigenvalue λ_0 . We begin with a mathematically rigorous lemma that this first numerical method is based on:

Lemma 9. *We fix any $m < 0$ and consider the eigenvalue equation (10). Let u be a not-identically-zero eigenfunction associated to the first eigenvalue λ_0 . Then u cannot attain zero at any value of t , and*

$$u(\ell + t) = u(\ell - t) \quad \text{for all } \ell \in \{a, \frac{3a+b}{4}, \frac{a+b}{2}, \frac{a+3b}{4}, b\}.$$

In particular,

$$u'(a) = u'(\frac{3a+b}{4}) = u'(\frac{a+b}{2}) = u'(\frac{a+3b}{4}) = u'(b) = 0.$$

Proof. Proposition 5 tells us that the eigenspace associated to the first eigenvalue λ_0 must be one dimensional. If u did not have all of the same symmetries as V as in Lemma 1, then there would be some $\ell \in \{a, \frac{3a+b}{4}, \frac{a+b}{2}, \frac{a+3b}{4}, b\}$ so that $u(\ell + t)$ and $u(\ell - t)$ are two linearly independent eigenfunctions associated to the same first eigenvalue λ_0 . This is a contradiction, implying the lemma. \square

Because multiplying u by a real scalar does not affect Equation (10), we may assume that

$$u(\frac{3a+b}{4}) = 1.$$

The numerical method is then to numerically solve Equation (10) for u with initial conditions

$$u(\frac{3a+b}{4}) = 1, \quad u'(\frac{3a+b}{4}) = 0$$

by some ODE solver (such as "NDSolve" in Mathematica), and find the value of λ that gives a periodic solution u , that is, that gives

$$u(a) = u(\frac{a+b}{2}) = u(b), \quad u'(a) = u'(\frac{a+b}{2}) = u'(\frac{a+3b}{4}) = u'(b) = 0, \quad u(\frac{a+3b}{4}) = 1, \quad u(t) > 0 \forall t \in [a, b],$$

or equivalently, by the symmetries of V in Equation (10) and by the symmetries of u in Lemma 9, that simply gives

$$(11) \quad u'(a) = u'(\frac{a+b}{2}) = 0.$$

Numerically finding this value of λ for various values of $m < 0$, one finds that it is always $m - 1$, verifying the primary numerical result.

Figure 3 demonstrates how this occurs, for the cases $m = -1$, -2 and -3 . In each case, the ODE solver produces a solution that satisfies Equation (11) precisely when $\lambda = m - 1$. When $\lambda \in (m - 1, m]$ (for example, $\lambda = m - 0.8$ as in Figure 3), the values of t ($\neq \frac{3a+b}{4}$) closest to $\frac{3a+b}{4}$ where $u'(t) = 0$ satisfy $|t - \frac{3a+b}{4}| < \frac{b-a}{4}$. When $\lambda \in [m - 2, m - 1]$ (for example, $\lambda = m - 1.2$ as in Figure 3), the

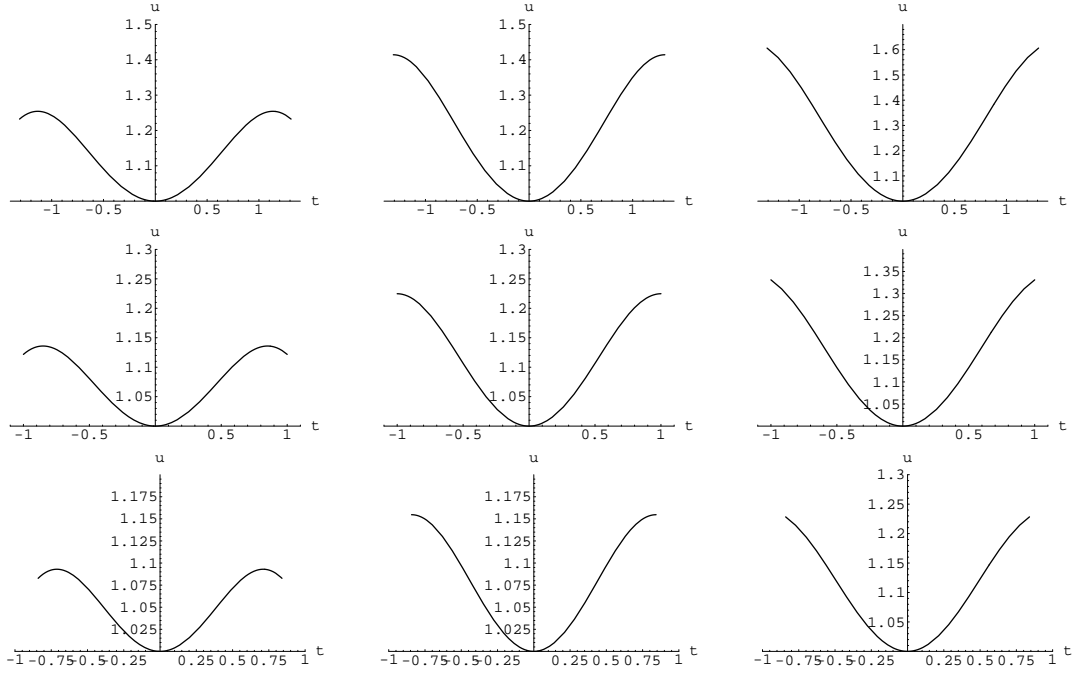


FIGURE 3. The function u computed numerically via the first method. In the first (resp. second, third) row, m is -1 (resp. -2 , -3). In the first (resp. second, third) column, λ is $m - 0.8$ (resp. $m - 1$, $m - 1.2$). In each case, the graph is drawn for $t \in [a, \frac{a+b}{2}]$ with $3b = -a = 1.3108$ (resp. 1.0 , 0.8428) for $m = -1$ (resp. -2 , -3).

values of t ($\neq \frac{3a+b}{4}$) closest to $\frac{3a+b}{4}$ where $u'(t) = 0$ satisfy $|t - \frac{3a+b}{4}| > \frac{b-a}{4}$. We need precisely $u'(\frac{a+b}{2}) = u'(a) = 0$, and this occurs exactly when $\lambda = m - 1$. This has been checked for numerous other values of $m < 0$ as well.

6. SECOND METHOD

The second method we present here is more complicated than the first one, but we wish to consider it for the following two reasons: 1) it does not use an ODE solver and the algorithm is independent of the first method above, thus it gives a second fully-independent confirmation of the numerical result; 2) it is a stronger method in that it also gives estimates for other eigenvalues of \mathcal{L}_0 , not just the first one.

As we saw in Proposition 3 and the remark just after Proposition 5, in addition to λ_0 , -1 and 0 are both also eigenvalues of \mathcal{L}_0 for all $m < 0$, and -1 and 0 are actually the second and third eigenvalues of \mathcal{L}_0 . The fact that this second method precisely estimates the second and third eigenvalues -1 and 0 gives us confidence that the method is accurately estimating λ_0 as well.

We choose a basis $\{\mathcal{B}_j = \mathcal{B}_j(t)\}_{j=1}^{\infty}$ for $\hat{\mathcal{F}}$ as

$$\mathcal{B}_1 = \frac{1}{\sqrt{b-a}},$$

$$\mathcal{B}_j = \sqrt{\frac{2}{b-a}} \cdot \cos\left(\frac{\pi j(t-a)}{b-a}\right) \quad \text{for even } j \in 2\mathbb{Z}^+,$$

$$\mathcal{B}_j = \sqrt{\frac{2}{b-a}} \cdot \sin\left(\frac{\pi(j-1)(t-a)}{b-a}\right) \quad \text{for odd } j \in 2\mathbb{Z}^+ + 1.$$

This is an orthonormal basis for $\hat{\mathcal{F}}$ with respect to the Euclidean L^2 norm on the interval $[a, b]$. Any $u \in \hat{\mathcal{F}}$ can be expanded as

$$u = \sum_{j=1}^{\infty} a_j \mathcal{B}_j$$

for constants $a_j \in \mathbf{R}$. The Rayleigh quotient characterization (9) then gives

$$\lambda_0 = \min_{\sum_{j \geq 1} a_j^2 > 0} \frac{\sum_{j,k \geq 1} a_j a_k \alpha_{jk}}{\sum_{j,k \geq 1} a_j a_k},$$

where

$$\alpha_{jk} = \int_a^b -\mathcal{B}_j \frac{d^2}{dt^2} \mathcal{B}_k dt - \int_a^b V \mathcal{B}_j \mathcal{B}_k dt.$$

The integrals $\int_a^b -\mathcal{B}_j \frac{d^2}{dt^2} \mathcal{B}_k dt$ can be explicitly computed as

$$\int_a^b -\mathcal{B}_j \frac{d^2}{dt^2} \mathcal{B}_k dt = \delta_{jk} \left[\frac{j}{2} \right]^2 \frac{4\pi^2}{(b-a)^2},$$

where δ_{jk} is the Kronecker-delta function and $\left[\frac{j}{2} \right]$ is the greatest integer less than or equal to $\frac{j}{2}$.

Many integrals $\int_a^b V \mathcal{B}_j \mathcal{B}_k dt$ must be computed numerically (by a numerical integrator, such as "NIntegrate" in Mathematica), but for each $n \in \mathbf{Z}^+$ ($n \geq 3$) more than half of the entries of the $n \times n$ matrix $(\int_a^b V \mathcal{B}_j \mathcal{B}_k dt)_{j,k=1}^n$ can be determined to be zero simply by using the symmetry properties of the functions V and \mathcal{B}_j . For example, $V(a+t) = V(a-t)$ and $\mathcal{B}_2(a+t) = \mathcal{B}_2(a-t)$, but $\mathcal{B}_3(a+t) = -\mathcal{B}_3(a-t)$, and so $\int_a^b V \mathcal{B}_2 \mathcal{B}_3 dt$ must be zero.

Let us list the eigenvalues of \mathcal{L}_0 in increasing order as

$$\lambda_0 < \lambda_1 = -1 < \lambda_2 = 0 < \lambda_3 \leq \lambda_4 \leq \dots \rightarrow +\infty.$$

Each eigenvalue appears in this list the same number of times as the dimension of its eigenspace. As noted in Proposition 4, $\lim_{j \rightarrow \infty} \lambda_j = +\infty$.

Remark. In fact, all eigenvalues have multiplicity at most 2. No eigenspace can contain three independent eigenfunctions, as \mathcal{L}_0 is a second-order linear ODE.

For each $n \in \mathbf{Z}^+$, the $n \times n$ matrix $(\alpha_{jk})_{j,k=1}^n$ is symmetric, so it also has real eigenvalues, which we list in increasing order as

$$\lambda_0^{(n)} \leq \lambda_1^{(n)} \leq \lambda_2^{(n)} \leq \dots \leq \lambda_{n-1}^{(n)}.$$

Rayleigh quotient characterizations for λ_j and $\lambda_j^{(n)}$ prove that

$$(12) \quad \lambda_j^{(j+1)} \geq \lambda_j^{(j+2)} \geq \lambda_j^{(j+3)} \geq \dots \geq \lambda_j.$$

Thus the limit $\lim_{n \rightarrow \infty} \lambda_j^{(n)}$ exists and is greater than or equal to λ_j . Further arguments with Rayleigh quotient characterizations give that in fact the limit is exactly equal to λ_j :

Theorem 10. $\lim_{n \rightarrow \infty} \lambda_j^{(n)} = \lambda_j$.

This theorem now provides us with our second numerical method for estimating λ_0 (and any other eigenvalue of \mathcal{L}_0) by simply finding the smallest eigenvalue (and other eigenvalues) of the matrix $(\alpha_{jk})_{j,k=1}^n$ for sufficiently large n . By the inequalities (12), it is clear that the estimates will be from above. Numerical results are shown in Table 1, and they again confirm the primary numerical result in this paper.

Theorem 10 is proven in [18]. The essential facts behind the proof of this result are well established and can be found in many sources ([3], [4], [21] for example), but we reference [18] because the result there is given in a situation most analogous to the one we have here.

Remark. Symmetries of the first eigenfunction can allow us to remove some \mathcal{B}_j , if we are only looking for the first eigenvalue λ_0 . If u is the eigenfunction for the first eigenvalue, then the symmetries of u in Lemma 9 imply that $u = \sum_{j \geq 1} a_j \mathcal{B}_j$ with $a_j = 0$ when $j \geq 2$ is not an integer multiple of four. Then we can more quickly estimate λ_0 by using subspaces of $\hat{\mathcal{F}}$ spanned by only \mathcal{B}_1 and \mathcal{B}_{4k} for $k \in \mathbb{Z}^+$. However, this shortcut will not work for estimating the other eigenvalues of \mathcal{L}_0 .

m	$3b = -a$	Lemma 6's lower bound for λ_0	Lemma 8's upper bound for λ_0	First method's estimate for λ_0	Second method's estimate for λ_0	Second meth.'s est. for λ_1	Second meth.'s est. for λ_2	Second meth.'s est. for λ_3, λ_4	Second meth.'s est. for λ_5, λ_6
-1/4	2.0137	-2.25	-1.0522	-1.25	-1.245	-0.992	0.00543	1.44	4.45
-1/2	1.656	-2.5	-1.3643	-1.5	-1.4994	-0.9987	0.00102	2.279	6.75
-1	1.3108	-3	-1.9137	-2	-1.999	-0.9993	0.00062	3.86	11.021
-2	1.0	-4	-2.9483	-3	-2.999	-0.9932	0.00615	6.94	19.26
-3	0.8428	-5	-3.964	-4	-3.999	-0.999	0.00069	9.943	27.3
-10	0.4849	-12	-10.988	-11	-10.999	-0.9974	0.00256	30.99	83.46
-20	0.34683	-22	-20.994	-12	-20.999	-0.983	0.0168	61.056	163.61

TABLE 1. Estimates for λ_0 and other eigenvalues of \mathcal{L}_0 (computed using the values $H = 1$ and $n = 13$).

REFERENCES

- [1] L. Barbosa and M. do Carmo, *Stability of hypersurfaces with constant mean curvature*, Math. Z. 185, 339-353 (1984).
- [2] L. Barbosa, J.M. Gomes and A. M. Silveira, *Foliation of 3-dimensional space form by surfaces with constant mean curvature*, Bol. Soc. Bras. Mat. 18, 1-12 (1987).
- [3] P. Bérard, *Spectral Geometry: Direct and Inverse Problems*, Lecture Notes in Math. 1207, Springer-Verlag (1986).
- [4] I. Chavel, *Eigenvalues in Riemannian Geometry*, Academic Press Inc., 1976.
- [5] S.-Y. Cheng, *Eigenfunctions and nodal sets*, Comment. Math. Helv. 51, 43-55 (1976).
- [6] J. Choe, *Index, vision number, and stability of complete minimal surfaces*, Arch. Rat. Mech. Anal. 109, 195-212 (1990).
- [7] J. Dorfmeister, F. Pedit and H. Wu, *Weierstrass type representation of harmonic maps into symmetric spaces*, Comm. Anal. Geom. 6, 633-668 (1998).
- [8] J. Dorfmeister and H. Wu, *Construction of constant mean curvature trinoids from holomorphic potentials*, preprint (2000).
- [9] M. Kilian, S-P. Kobayashi, W. Rossmann and N. Schmitt, *Constant mean curvature surfaces with Delaunay ends in 3-dimensional space forms*, preprint, math.DG/0403366v2 (2004).
- [10] N. Korevaar, R. Kusner and B. Solomon, *The structure of complete embedded surfaces with constant mean curvature*, J. Differential Geom. 30, 465-503 (1989).
- [11] R. Kusner, R. Mazzeo and D. Pollack, *The moduli space of complete embedded constant mean curvature surfaces*, Geom. Funct. Anal. 6, 120-137 (1996).
- [12] R. Mazzeo and F. Pacard, *Bifurcating nodoids*, Topology and geometry, Contemp. Math., vol. 314, Amer. Math. Soc., 2002, pp. 169-186.
- [13] R. Mazzeo and F. Pacard, *Constant mean curvature surfaces with Delaunay ends*, Comm. Anal. Geom. 9, No. 1, 169-237 (2001).
- [14] R. Mazzeo, F. Pacard and D. Pollack, *The conformal theory of Alexandrov embedded constant mean curvature surfaces in \mathbb{R}^3* , preprint, math.DG/0110099 (2001).
- [15] F. Pacard, *personal communication*.
- [16] K. Polthier, *JavaView software, version 2.21*, <http://www-sfb288.math.tu-berlin.de/vgp/javaview/>, April 2003.
- [17] J. Ratzkin, *An end-to-end gluing construction for surfaces of constant mean curvature*, doctoral thesis, University of Washington (2001).
- [18] W. Rossmann, *The Morse index of Wente tori*, Geom. Dedicata 86, 129-151 (2001).
- [19] N. Schmitt, *Constant mean curvature trinoids*, preprint, math.DG/0403036, 2004.
- [20] N. Schmitt, *cmclab software*, <http://www.gang.umass.edu/software> and <http://tmugs.math.metro-u.ac.jp/>
- [21] H. Urakawa, *Geometry of Laplace-Beltrami operator on a complete Riemannian manifold*, Advanced Studies in Pure Mathematics, Progress in Differential Geometry 22, 347-406 (1993).

WAYNE ROSSMAN: Department of Mathematics, Faculty of Science, Kobe University, Rokko, Kobe 657-8501, Japan.
E-mail: wayne@math.kobe-u.ac.jp *web page:* www.math.kobe-u.ac.jp